The dynamics of hydrogen atoms in the hydrogen bonds of carboxylic acid dimers

1989 J. Phys.: Condens. Matter 1 9609

(http://iopscience.iop.org/0953-8984/1/48/011)

J. Phys.: Condens. Matter **1** (1989) 9609–9622. Printed in the UK

The dynamics of hydrogen atoms in the hydrogen bonds of carboxylic acid dimers

A J Horsewill and A Aibout
Department of Physics, University of Nottingham, University Park, Nottingham NG7 2RD, UK

Received 6 July 1989

Abstract. The techniques of pulsed NMR spectroscopy and inelastic neutron scattering (INS) have been employed to study the coordinated motion of hydrogen atoms in the hydrogen bonds of carboxylic acid dimers. The proton spin–lattice relaxation time T_1 has been measured at two frequencies in diglycolic acid and suberic acid and the reorientation rate in diglycolic acid has been measured directly by quasi-elastic neutron scattering. Furthermore T_1 data have been collected on benzoic acid, terephthalic acid and malonic acid at different spectrometer frequencies to those in earlier published data. The NMR and INS data have been successfully fitted to a new model proposed by Skinner and Trommsdorff in which the low-temperature dynamics, under the influence of an asymmetric double-minimum potential, are dominated by phonon-assisted tunnelling while that at high temperature follows an Arrhenius rate law. Fitting the T_1 data at two different frequencies simultaneously with the INS data restricts the possible values of the parameters in the theory to a narrow range. The values of the parameters, particularly the barrier heights and asymmetry, are discussed in terms of the known molecular structures. Further discussion centres upon some new NMR data of the proton dipolar relaxation time T_{1D} in terephthalic acid and benzoic acid.

1. Introduction

Systems in which hydrogen atoms undergo motion within a hydrogen bond have created interest in recent years. Some of this has been generated because the system has the potential for displaying quantum mechanical tunnelling behaviour. Furthermore the motion provides an example of a particularly simple chemical reaction and may be of interest in the study of the quantum mechanical aspects of proton transfer reactions and indeed more complicated molecular rearrangements. Other molelcular dynamical systems that have been studied hitherto and display clear quantum mechanical tunnelling in the solid state include CH_3, NH_3, CH_4 and NH_4 reorientation, the translational tunnelling associated with the diffusion of hydrogen in metals [1], and rotational tunnelling of molecular hydrogen [1a]. In one case, namely that of methyl (CH_3) reorientation, considerable progress has been made in recent years towards achieving a fundamental understanding of the smooth transition from quantum to classical mechanics with increase in temperature [2].

Carboxylic acids commonly form centrosymmetric dimers in the solid state in which a ring structure is formed by two hydrogen bonds. This is illustrated in figure 1. This is true also of dicarboxylic acids, the crystal structures of which commonly consist of continuous polymeric chains of molecules bound by hydrogen bond dimers. Within a

0953-8984/89/489609 + 14 $02.50

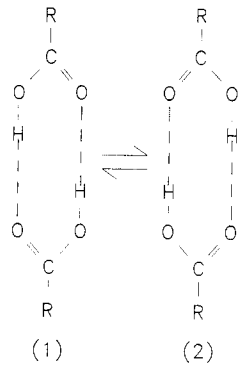

Figure 1. The molecular structure of carboxylic acid dimers.

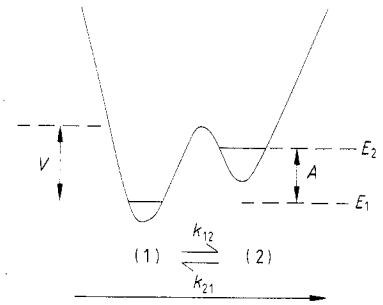

Figure 2. Potential energy diagram for the coordinated motion of two hydrogen atoms in the hydrogen bonds of carboxylic acid dimers.

single dimer unit two conformations, labelled 1 and 2, are possible, so the potential energy of the system with respect to the hydrogen atom position has a double minimum. In the solid state the effect of neighbouring molecules is to break the symmetry of the potential, so the two potential wells may in general be of unequal depth. The resulting asymmetry in the double minimum is designated A (see figure 2). It is possible for the hydrogen atoms to undergo motion within each hydrogen bond. In this model the motion of the two hydrogen atoms is coordinated and in the plane of the dimeric ring structure. In this way the perturbations to the electronic structure within the dimer resulting from the hydrogen atom motion are minimised and to a good approximation only one spatial coordinate is required to describe the dynamics. The motion of atoms in one dimer is assumed here to be independent of motion within another dimer. Experimental evidence that the essential qualitative aspects of this picture correctly describe the dynamics in these systems has been provided by neutron scattering. For example, measurement of the Q-dependence of the quasi-elastic neutron scattering (QENS) spectrum recorded on single crystals of terephthalic acid [3] discriminated against an alternative model proposed by Furic [4] in which the suggestion was made that the two conformers interchanged by rotation of the whole ring structure about an axis parallel to the hydrogen bonds through the center of the dimer.

A number of carboxylic acid dimer systems have been studied in recent years by NMR spectroscopy and inelastic neutron scattering (INS) [5–9]. The models used to explain the dynamics were however often less than satisfactory particularly in the low-temperature region. Experimentally observed deviations from the classical models proposed, for example the low activation energies at low temperature, were invariably assigned only qualitatively to a tunnelling mechanism. Other deficiencies in the models presented included their inability to account quantitatively for the frequency independence of the proton spin–lattice relaxation time in some materials (for example terephthalic acid).

Recently Skinner and Trommsdorff [10] have developed a new theory for the dynamics in which the motion in the low-temperature regime is dominated by phonon-assisted tunnelling. In this model the dynamics at high temperature is described by thermally activated hopping. In both regimes their model accommodated the asymmetric nature of the double-minimum potential. When applied to the NMR data on benzoic acid and the results of optical measurements the model met with quantitative success. In this paper we present the results of a new series of NMR and INS measurements on carboxylic acid dimers. These data have been analysed successfully according to

Skinner and Trommsdorff's model. Furthermore the published data for other systems have also been re-analysed in the light of this new theory.

Our new measurements have been performed on diglycolic acid and suberic acid using the techniques of NMR and INS. The NMR data include measurements of the proton spin–lattice relaxation time T_1. New NMR data have also been collected upon systems that have been studied before, namely terephthalic acid, benzoic acid and malonic acid. In these cases the previously published data have been supplemented by new T_1 measurements at different frequencies and with measurements of the proton dipolar relaxation time T_{1D}. As will become apparent, the provision of frequency-dependent T_1 data provides a further test of Skinner and Trommsdorff's theory and indeed restricts the possible values of parameters in the theory to a narrow range.

2. Experimental details

All experimental samples were obtained commercially from the Aldrich Chemical Company and studied in the form of crystalline powders.

2.1. Nuclear magnetic resonance spectroscopy

The relaxation time measurements were made using pulsed NMR spectroscopy. The proton spin–lattice relaxation time was measured using the saturation-recovery technique, saturation of proton magnetisation having been achieved initially with a train of typically eight $\pi/2$ pulses. Measurements were made at 21 or 22 MHz and 100.5 MHz. The sample temperature was accurate in setting and control to ± 0.5 K. Measurements of the proton dipolar relaxation time T_{1D} were made using the three-pulse sequence developed by Jeener and Broekaert [11]. This pulse sequence is described as follows; $(\pi/2)_0$–t_a–$(\pi/4)_{90}$–t_b–$(\pi/4)_{90}$. Here $\pi/2$ and $\pi/4$ represent the tipping angles of the pulses and the subscripts represent the relative phases of the RF pulses. In this sequence the time interval t_a was typically 15 μs and was chosen to maximise the intensity of the echo after the third pulse. The value of T_{1D} was determined by plotting the decay of the echo in question as a function of time interval t_b. The decay was exponential to within experimental error. These particular measurements were performed at the spectrometer frequency of 22 MHz.

2.2. Neutron scattering spectroscopy

Neutron scattering measurements were performed upon diglycolic acid using the pulsed neutron source ISIS at the Rutherford Appleton Laboratory. The quasi-elastic neutron scattering spectra were recorded as a function of temperature on the IRIS spectrometer and collected in the Q-range from 1.0 to 1.85 Å^{-1}. IRIS is an inverted-geometry time-of-flight spectrometer which employs pyrolytic graphite crystal analysers in near-back-scattering geometry. The resolution of the spectrometer is approximately 15 μeV. The sample of thickness 1 mm was mounted in an aluminium slab-shaped container and the temperature was set and controlled to an accuracy of 1 K. Each spectrum was recorded for a period of 14 h with the neutron source ISIS running at 90 μA. Ideally the analysis of the data would use a procedure in which each QENS spectrum was fitted to a model spectrum consisting of a quasi-elastic Lorentzian line and an elastic line both convoluted with the measured spectrometer resolution function. Since the intensity of the quasi-elastic line was small by comparison with both the elastic line and the background such

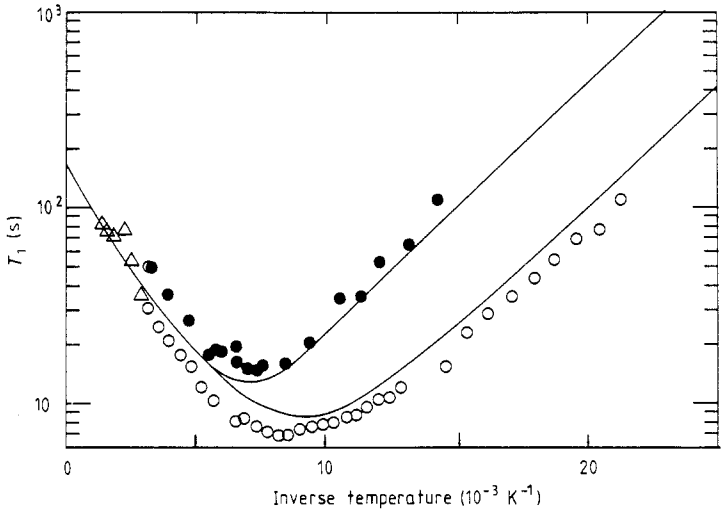

Figure 3. *Diglycolic acid.* The temperature dependence of T_1 at 21.04 MHz (open circles) and 100.54 MHz (full circles). The full curves show the fit of the T_1-data to the theory of Skinner and Trommsdorff at the two measured frequencies and the open triangles are determined from the QENS data.

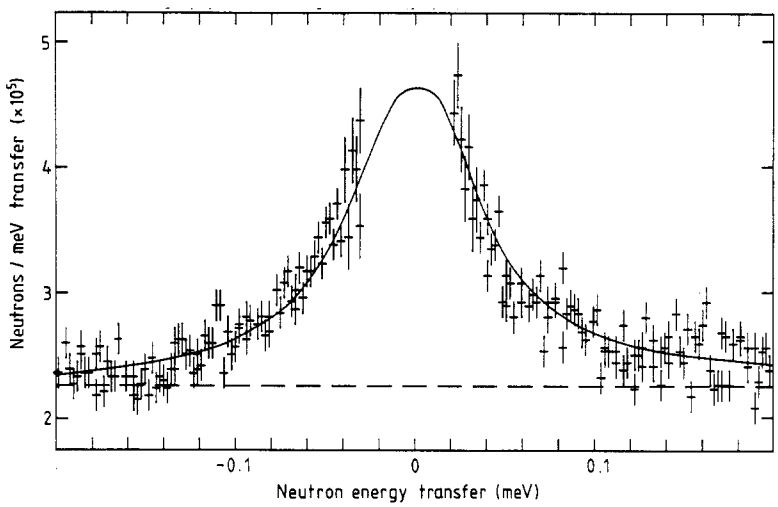

Figure 4. The quasi-elastic neutron scattering spectrum of diglycolic acid recorded on the IRIS spectrometer at 300 K. See text for details.

a full analysis of the data has not been possible with the available statistics. We have made a preliminary analysis by preparing the data prior to the fitting procedure by subtracting the elastic line from each spectrum and summing all detectors in the Q-range reported above. The elastic line representing the resolution function was recorded using a sample of diglycolic acid at a temperature of $\simeq$70 K. Under these conditions no QENS or INS was evident within the range of energy transfer and resolution in question. In order to extract the dynamical data the resulting spectrum, of which figure 4 is an example, was then fitted to a single quasi-elastic Lorentzian line convoluted with the resolution function.

3. Theory of hydrogen bond dynamics and spin–lattice relaxation

We provide here a summary of the essential features and results of theory for hydrogen bond dynamics developed by Skinner and Trommsdorff [10]. Full details of the model are provided in their paper.

The hydrogen atoms move in a coordinated fashion within the ring completed by the two hydrogen bonds. Each hydrogen atom moves within the confines of its own hydrogen bond. They each experience an asymmetric double-minimum potential as sketched in figure 2, in which the height of the potential barrier between the minima is designated V and the asymmetry of the potential is A. In this diagram the coordinate describing the position of the hydrogen atoms is plotted along the horizontal axis and this coordinate is coupled to the vibrations of the crystal. The dynamics between the two wells is governed by the rate constants k_{12} and k_{21} for the forward and reverse motions respectively and these should satisfy the requirements of detailed balance. At low temperature the motion is dominated by phonon-assisted tunnelling, the rate constants being

$$k_{21}^{\mathrm{L}} = k_{21}^{0}(n(\omega_{21}) + 1) \tag{1}$$

$$k_{12}^{\mathrm{L}} = k_{21}^{0}(n(\omega_{21})) \tag{2}$$

where

$$n(\omega) = 1/(\exp(\hbar\omega_{21}/kT) - 1). \tag{3}$$

Here a Debye density of states has been assumed and the energy $\hbar\omega_{21} = (E_1 - E_2) \simeq A$, the asymmetry. k_{21}^{0} is a constant and the superscripts L designate the low-temperature regime. The functional form of k_{21}^{0} is not used explicitly in the data-fitting procedure in this paper but is given here for completeness:

$$k_{21}^{0} = (3\pi/2)p^2(J/\hbar\omega_{\mathrm{D}})^2\omega_{21}. \tag{4}$$

In this equation p is a dimensionless phonon coupling parameter, J the tunnelling matrix element and ω_{D} is the Debye cut-off frequency. In the high-temperature regime the dynamics is determined by thermally activated barrier crossing and is written in Arrhenius form as follows:

$$k_{12}^{\mathrm{H}} = (1/\tau_0)(\exp(-V/kT)) \tag{5}$$

$$k_{21}^{\mathrm{H}} = (1/\tau_0)\{\exp[-(V - A)/kT]\}. \tag{6}$$

Again the asymmetry of the barrier is accommodated and the superscript H designates the high-temperature regime. In the intermediate-temperature region the values of the rate constants are interpolated in the following way:

$$k_{21} = k_{21}^{\mathrm{L}} + k_{21}^{\mathrm{H}} \qquad k_{12} = k_{12}^{\mathrm{L}} + k_{12}^{\mathrm{H}}. \tag{7}$$

The dynamics is then determined by the correlation time, τ_{c} where $1/\tau_{\mathrm{c}}$ is the reorientation rate and

$$1/\tau_{\mathrm{c}} = k_{12} + k_{21}. \tag{8}$$

The measurements of T_1 are interpreted according to the formula originally given by Look and Lowe [12] for proton transfer between inequivalent sites:

$$T_1 = (1 + a)^2/aCB(\tau_{\mathrm{c}}) \tag{9}$$

where

$$B(\tau_{\mathrm{c}}) = \tau_{\mathrm{c}}/(1 + \omega_0^2\tau_{\mathrm{c}}^2) + 4\tau_{\mathrm{c}}/(1 + 4\omega_0^2\tau_{\mathrm{c}}^2) \tag{10}$$

$$a = \exp(A/kT). \tag{11}$$

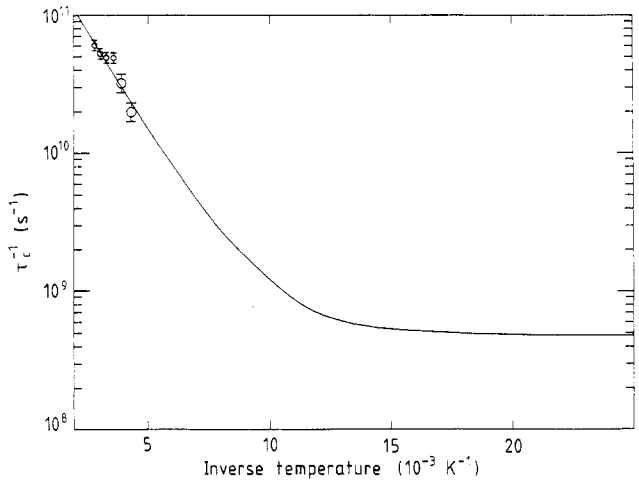

Figure 5. The temperature dependence of the reorientation rate τ_c^{-1} in diglycolic acid. Circles: experimental points from QENS. Full curve: deduced from the model of Skinner and Trommsdorff.

Here C is a constant determined by a lattice sum of dipole–dipole matrix elements and $\omega_0 = 2\pi\nu_0$ where ν_0 is the spectrometer frequency.

4. Results and discussion

Measurements of hydrogen bond dynamics in diglycolic acid and suberic acid are reported here for the first time. We have also measured T_1 (and T_{1D} in two cases) for terephthalic acid, benzoic acid and malonic acid at different spectrometer frequencies to the original publications. As will become apparent the provision of T_1-data at two frequencies is important in determining accurate values for the parameters in the model thoery. The results obtained will be discussed in turn.

4.1. Results

4.1.1. Diglycolic acid (2,2'-oxydiacetic acid; $O(CH_2CO_2H)_2$). The temperature dependence of T_1 has been measured at 21.04 MHz and 100.54 MHz. The data are presented in figure 3. Minima in T_1 are observed at both frequencies, they occur at temperatures of 116 K at 100 MHz and 99 K at 21 MHz. Asymmetry in the activation energies either side of the T_1-minimum is evident. The value of T_1 recorded at the minimum at 21 MHz was 7 s.

The QENS spectra have been recorded on the IRIS spectrometer as a function of temperature. As an example one QENS spectrum is shown in figure 4 recorded at a temperature of 300 K. The elastic line has been subtracted from these data and the immediate vicinity of the elastic region has been omitted from the diagram for reasons of clarity. The full curve is the best-fit model spectrum. The rate of hydrogen motion is given by the half-width of the Lorentzian QENS line and in figure 5 the experimental values of this quantity are shown as a function of temperature in the range 220 K to 320 K.

4.1.2. Suberic acid ($HO_2C(CH_2)_6CO_2H$). T_1-data recorded at spectrometer frequencies of 100.54 MHz and 21 MHz are presented in figure 6. Minima in T_1 are observed at 105 K

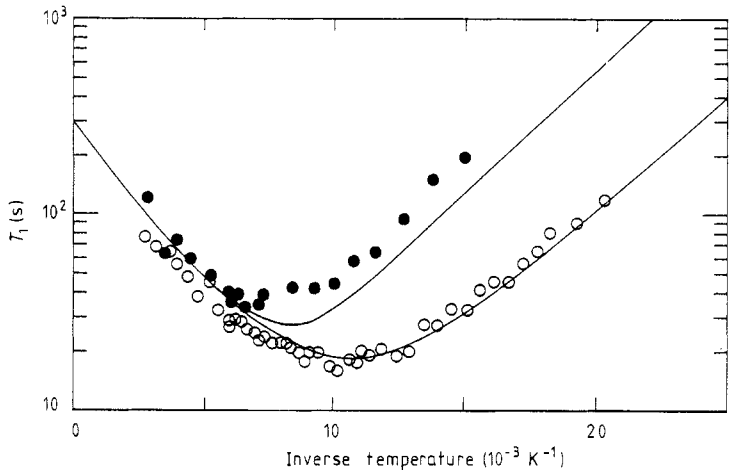

Figure 6. *Suberic acid.* This temperature dependence of T_1 as in figure 3.

and 77 K respectively for the two frequencies. The value of T_1 recorded at the minimum and at 21 MHz is ≃17 s, which is itself relatively shallow and reflects spin diffusion within the proton spin reservoir containing the relatively large number of non-carboxylic acid protons in the molecule.

4.1.3. Benzoic acid ($C_6H_5CO_2H$). Previous measurements of T_1 in this material were made by Nagaoka *et al* [6, 7] at 59.53 MHz. We have measured T_1 at 22.0 MHz and these new results together with the previous measurements are presented in figure 7. The minima occur at 48 K at 22 MHz and 64 K at 59.53 MHz. Neutron scattering data published by Ernst *et al* [13] are also presented on this diagram as triangles; the details of these will be given in a later section. Measurements of T_{1D} have been made and are presented in the figure. A minimum is observed at ≃45 K, a very similar temperature to the minimum in T_1 recorded at 22 MHz. The activation energies either side of the T_{1D} minimum are also asymmetric.

4.1.4. Terephthalic acid (C_6H_4-1,4-$(CO_2H)_2$). Terephthalic acid crystallises in two forms, I and II, identified in the x-ray structure determination by Baily and Brown [19]. There was evidence to suggest that type I was the more stable at low temperature. Previous NMR measurements were made by Meier *et al* [5] at 100 MHz and 25 MHz. We have measured T_1 at 21 MHz and T_{1D}. The new data and the 100 MHz data are presented in figure 8 together with the QENS data of Ernst *et al* [14]. Asymmetry in the activation energies either side of the T_1-minimum (at ≃83 K) is evident and it is notable that the frequency dependence of the data is only slight. We shall return to these features in the discussion. The new 21 MHz data were collected for a powder and no attempt was made to exclude type II crystals. These data are however in excellent agreement with those of Meier *et al*. Measurements of T_{1D} are also presented in the figure. In this case two minima are observed at 82 K and 16 K.

4.1.5. Malonic acid ($HO_2CCH_2CO_2H$). Previous measurements were made at 90 MHz by Idziak and Pislewski [8]. We have measured T_1 at 21 MHz. The new data and the earlier measurements are presented together in figure 9. The minimum in T_1 occurs at 130 K at 21 MHz and at 150 K at 90 MHz. The respective values of T_1 at the minimum are ≃22 s and ≃30 s.

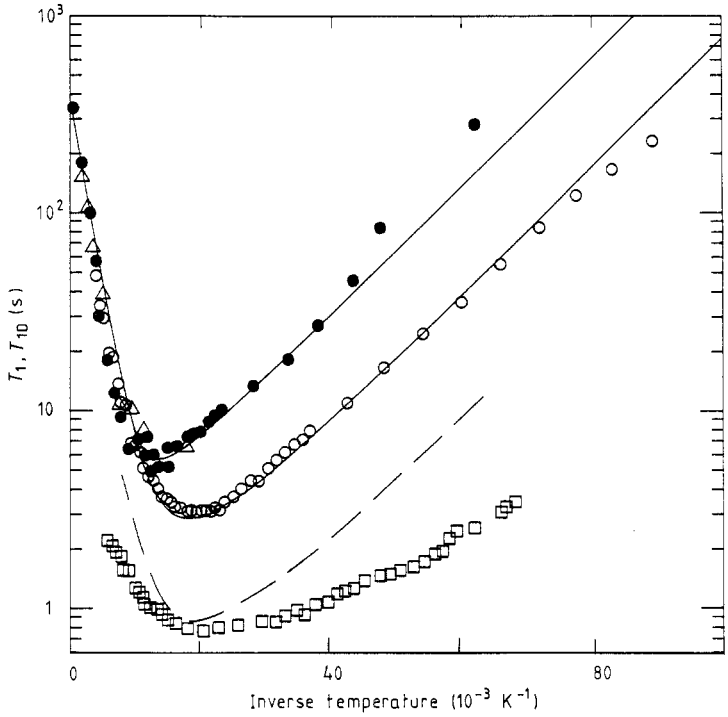

Figure 7. *Benzoic acid.* The temperature dependence of T_1 at 22.01 MHz (open circles: this work) and 59.53 MHz (full circles: from [6]). The QENS data (open triangles) are from [13]. T_{1D}-data are presented as open squares. The full curves represent the modelled dependence of T_1 at the two measured frequencies. The broken curve is the model prediction for T_{1D}.

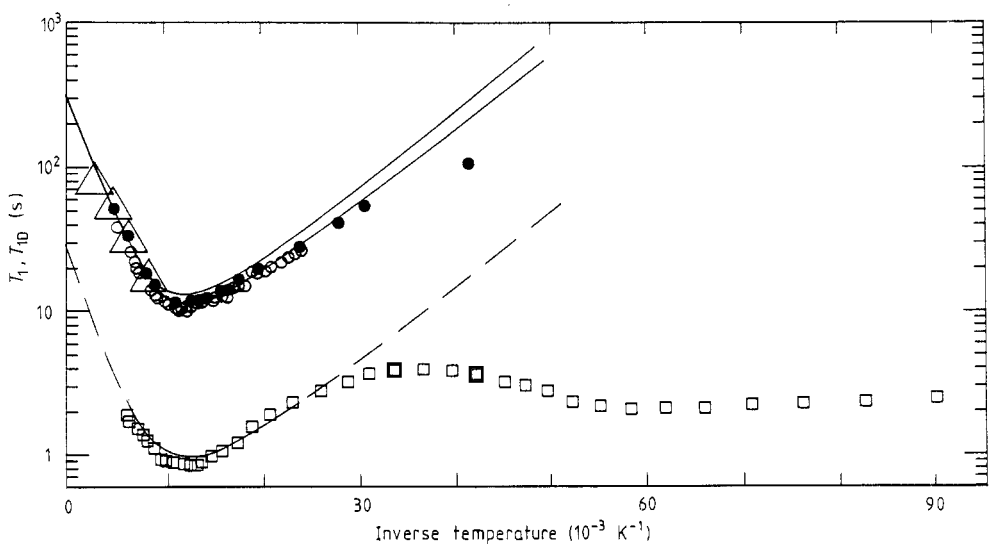

Figure 8. *Terephthalic acid.* The temperature dependence of T_1 at 21 MHz (open circles: this work) and 100 MHz (full circles: from [5]). The QENS data (open triangles) are from [14]. Otherwise, as for figure 7.

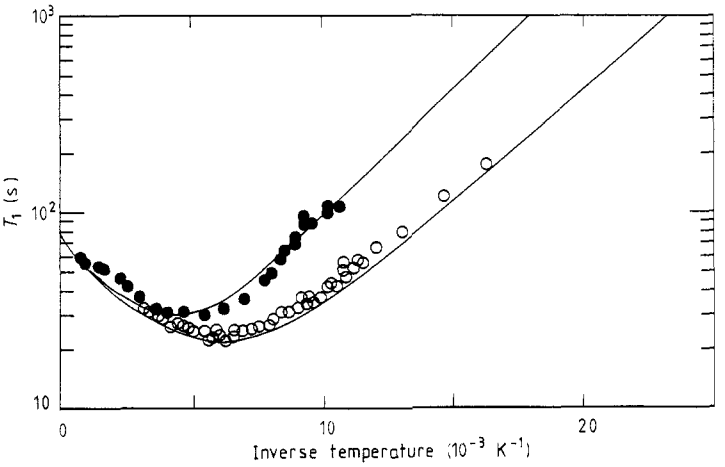

Figure 9. *Malonic acid.* The temperature dependence of T_1 at 21.03 MHz (open circles: this work) and 90 MHz (full circles: from [8]).

4.2. The analysis of T_1 and QENS data

The model of Skinner and Trommsdorff [10] has been fitted to the experimental T_1 and QENS data for all the materials studied. There are four independent parameters in the theory for the hydrogen bond dynamics, namely V, A, τ_0 and k_{21}^0. Furthermore the value of C is also a parameter in the analysis of T_1. The two full curves in figure 3 and figures 6 to 9 represent the best fits that could be found to the data and depict the calculated dependence of T_1 at the two measured frequencies. For convenience and to illustrate the quality of the fits to the model, the neutron scattering data (where available) have been accommodated in these figures. The QENS data on the reorientation rate have been converted here to the equivalent value of T_1 (at the highest measured frequency) using the formulae (9)–(11) and are plotted as triangles. The procedure employed in the fitting procedure was automated using a microcomputer although convergence towards the best fit was judged by eye. The best-fit parameters are presented in table 1.

The data for T_1 at two different frequencies and the neutron scattering data were simultaneously employed in determining the best-fit parameters. Use of the three data sets restricted the possible values of the parameters. For example, in order to ensure that the values of the reorientation rate derived from QENS were consistent with those derived from T_1, the value of the constant C was closely confined. Furthermore the provision of T_1-data at two different frequencies provided further discrimination in the values of the parameters. The convergence to the best fit was not judged according to a full least-squares analysis, so a full statistical analysis of the reliability of the parameters in the table has not been performed. However, it has been possible to assess the sensitivity of the fitted curve to each parameter. Reasonable fits can be accommodated for the following percentage range in each parameter: V and A, 3%; C, 6%; k_{21}^0, 20%; and τ_0, 12%.

As the figures show, the model of Skinner and Trommsdorff provides a very satisfactory account of the dynamics of hydrogen bonds in carboxylic acid dimers. The range of values for the potential V and the asymmetry A extend from 500 K to 920 K and from 78 K to 320 K respectively for the materials studied. The model successfully accounts for the weak frequency dependence of the T_1-data for terephthalic acid which had not been explained in previous theoretical models. The agreement between the data derived

Table 1.

	θ_{min} (K)		V	A	τ_0	k_{21}^0	C	r(O ··· H–O)	r(C–O)		r(C=O)
	21 MHz	100 MHz	(K)[a]	(K)[a]	(10^{-12} s)	(10^8 s^{-1})	(10^8 s^{-2})	(Å)[b]	(Å)	q	(Å)
Diglycolic acid	99	116	920	310	4.0	4.8	7.0	2.67	1.300		1.226
										0.059	
Suberic acid	77	105	800	290	4.0	4.0	4.0	2.65	1.309		1.227
										0.065	
Malonic acid	130	170[c]	750	320	50.0	5.0	1.7	2.71	1.29		1.24
										0.040	
								2.68	1.31		1.22
										0.071	
Benzoic acid	48	73[c]	500	78	6.0	2.8	2.84	2.627	1.268		1.258
										0.0079	
Terephthalic acid	83	83	600	130	10.0	21.0	3.5	2.608	1.272		1.262[d]
										0.0079	

[a] 1 K = 8.31×10^{-3} kJ mol^{-1} = 0.695 cm^{-1}.
[b] Crystallographic data from [16] to [20].
[c] Calculated from the model.
[d] Type I crystal.

from neutron scattering and those from NMR is particularly good, which is well demonstrated by the case of benzoic acid in figure 7. The parameter values for benzoic acid reported here are slightly different to those reported in the original paper by Skinner and Trommsdorff. Their published values have been improved slightly and now the fit agrees more closely with the new 22 MHz data as well as the original QENS and NMR data.

The full curve in figure 5 portrays the modelled dependence of the reorientation rate τ_c^{-1} as a function of $1/T$ for diglycolic acid; the INS data are superimposed for direct comparison. The parameters are the same as those used to calculate the model dependence of T_1 shown in figure 3. Figure 5 clearly illustrates the dynamics in the low- and high-temperature regimes. At high T, where the dynamics is dominated by thermally activated hopping, the activation energy is determined by the values of V and A. From the gradient of the line in the region where INS is sensitive, the value of the activation energy is 700 K. At low temperature, where the motion is dominated by phonon-assisted tunnelling, the reorientation rate is almost constant. Comparison of figures 3 and 5 illustrates that the low-temperature gradient exhibited by T_1 is determined by the term $(1 + a)^2/a$ in Look and Lowe's expression equation (9). The effect of this term on the value of T_1 is further illustrated by the gradient of the T_1-curve in the region of the INS data (220 K–320 K). Here the gradient is only 515 K, significantly smaller than the true value, 700 K, of the activation energy.

For malonic acid Idziak and Pislewski [8] assumed a classical model for the hydrogen motion which was very similar to the high-temperature regime in the theory presented here. The essential difference was that they omitted the phonon-assisted tunnelling mechanism. Although their 90 MHz data seemed to suggest that the absolute value of the gradient of T_1 versus $1/T$ observed at low temperature was greater than that observed at high temperature this is not borne out in our 21 MHz data. Attempts to use the parameters in [8] to describe both sets of T_1-data in the absence of phonon-assisted tunnelling led to failure since a very steep rise in the gradient of T_1 versus $1/T$ was predicted at low temperature. Our fits of the malonic acid data to the theory of Skinner and Trommsdorff are by contrast reasonably successful. The values of V and A are within the typical range observed in other materials studied but the value of τ_c is somewhat larger; this, however, is to be expected since the minimum in T_1 occurs at higher temperature. This particular example is one for which there is a need for neutron scattering data to confine more closely the values of the parameters in the theory.

The relative insensitivity of T_1 to the NMR spectrometer frequency in terephthalic acid reflects the fact that the value of k_{21}^0 is relatively high compared with that for the other materials and that the dynamics is dominated by phonon-assisted tunnelling even at relatively high temperatures. By comparison benzoic acid has a minimum in T_1 at lower temperature and a lower asymmetry; however, these data retain more of their dependence upon frequency since the value of k_{21}^0 is smaller. Further calculations within the model for benzoic acid show, however, as expected, that T_1 progressively loses its dependence upon frequency as ν_0 is decreased. This trend is demonstrated experimentally by the T_{1D}-data, the subject of the next sub-section. According to (4) k_{21}^0 depends upon three constants, namely J, p and ω_D, in addition to A. These are not known independently so it is not currently possible to interpret the fitted values in table 1 in terms of them.

4.3. The temperature dependence of T_{1D}

A rigorous analytical expression for $T_{1D}(\tau_c)$ has not been given since the region $\omega\tau_c \simeq 1$ falls between the weak- and strong-collision limits. However Lauer *et al* [15] have

used a heuristic approach to provide an expression for T_{1D}. We have made an *ad hoc* modification to this to accommodate the asymmetry in the potential wells to give the following:

$$T_{1D} = (1 + a)^2/aD(\tau_c) \qquad D(\tau_c) = C_{1D}J(\omega_0) + C_{2D}J(2\omega_0) + C_{3D}J(\omega_L) \tag{12}$$

where

$$J(\omega) = \tau_c/(1 + \omega^2\tau_c^2)$$

and ω_L is the resonance frequency in the local (molecular) field experienced by the protons. The values of the constants C_{iD} may be of the order of the constant C appearing in the T_1-theory. Since ω_L is of order (say) $100 \times 10^3\ s^{-1}$, and since it has been noted that the frequency dependence of T_1 becomes progressively independent of ω_0 as the frequency is decreased, it may be deduced from the similarity in the functional forms of T_1 and T_{1D} that there will be a strong similarity between the temperatures at which T_1(21 MHz) and T_{1D} are a minimum. A qualitative assessment of the data in figures 7 and 8 shows that this expectation is indeed upheld. Furthermore the broken curve in those figures is the functional form of T_{1D} according to (12). Here the parameters leading to the calculation of τ_c are identical to those employed in table 1 and for simplicity we have assumed that $C = C_{1D} = C_{2D}$. The values of C_{3D} are as follows: $3 \times 10^9\ s^{-2}$ for benzoic acid and $22 \times 10^9\ s^{-2}$ for terephthalic acid. ω_L was chosen to be $1 \times 10^5\ s^{-1}$ but the curves are relatively insensitive to this parameter. In both cases the temperatures of the minima in T_{1D} are correctly predicted; however, the approximations leading to (12) may be responsible for the difference between the calculated and experimental activation energies.

One distinctive feature of the terephthalic acid T_{1D}-data is the additional minimum at 16 K. This occurs, according to the model, when the reorientation rate τ_c^{-1} is approximately $2 \times 10^9\ s^{-1}$ and relatively independent of the temperature. There does not appear to be any corresponding minimum in T_1; experimentally this remains very long to low temperature. The origin of this minimum is not known and requires further investigation. At low temperature one may question the validity of the assumption that the dynamics of the dimers remain independent of each other.

4.4. Interpretation and correlation of best-fit parameters with molecular structure

In table 1 the experimental best-fit parameters for a fit to the theory of Skinner and Trommsdorff are supplemented by data relating to the molecular structure of the dimer, namely the hydrogen bond distance r(O–H $\cdots$ O) and the single and double carbon–oxygen bond distances r(C–O) and r(C=O). These data, collected at room temperature, are from x-ray and neutron diffraction structure determinations in references [16] to [20]. The differences in the lengths of the C–O and C=O bonds are also summarised in table 1 by an asymmetry parameter $q = (r(\text{C–O}) - r(\text{C=O}))/r_{mean}$ where r_{mean} is the mean carbon–oxygen bond length. Furthermore it was expedient to define a parameter that summarises the global aspects of the T_1-data. To this end two columns are provided in the table for the temperature θ_{min} at which T_1 is a minimum at spectrometer frequencies of 21 MHz and 100 MHz respectively. These are convenient parameters since 100 MHz is sufficiently high to ensure that the relaxation is frequency dependent in most materials; by contrast 21 MHz is a frequency below which θ_{min} is almost independent of frequency. Unlike in the other materials represented in the table the two carboxylic acid groups in the molecule of malonic acid are not related by symmetry, so they are not necessarily

dynamically equivalent. The crystallographic data for both dimers are presented in table 1 and they are similar in dimension. The dynamical data presented in figure 9 are consequently expected to represent a convolution of two slightly different species.

For the purposes of discussion and to establish a connection between structural features of the hydrogen bond dimers and the dynamical parameters it will be convenient to partition the materials into two groups. The first, labelled (i), consists of benzoic and terephthalic acids and the second, (ii), consists of diglycolic, suberic and malonic acids. The members of group (i) both have the shortest hydrogen bond distances, r(O–H $\cdots$ O), and the lowest temperatures, θ_{min} (100 MHz). The comparatively low value of the O–H $\cdots$ O distances in group (i) also correlate with the potential barrier height, V, and asymmetry, A, since these are also the lowest values in the table. Furthermore group (i) has the smallest asymmetry q between the two carbon–oxygen distances by a factor of eight compared with group (ii).

When the hydrogen atoms undergo coordinated motion in the hydrogen bond dimer there is a change in the electronic structure and atomic arrangement within the dimer. For example a C=O bond changes in to a C–O bond and vice versa and the barrier height, V, reflects the redistribution of electronic charge as a function of proton coordinate. The asymmetry in the potential, A, is determined by the asymmetry in the inter-molecular environment and may also reflect coupling or interactions between pairs of dimers. In cases where the asymmetry, q, in the carbon–oxygen bond lengths is small then one may envisage that the description of a carbon–oxygen 'double' or 'single' bond becomes less distinct with an appropriate delocalisation of charge around the dimer ring. In such circumstances the observed correlation between the lowest observed barriers and the lowest asymmetry, q, becomes understandable since the extent to which the electronic distribution is perturbed as a function of proton coordinate is somewhat less. Similar comments apply to the correlation between the shortest hydrogen bonds and the lowest barrier heights. This is the first time to the authors' knowledge that such correlations between the dynamical parameters, the barrier height and shape, and the molecular structure have been observed. Their existence suggests the possibility of a universal law for double proton transfer and implies that the total number of independent parameters in such a theory is somewhat less than the total number quoted in the table. Alternatively the correlations may reflect the time-average nature of the x-ray diffraction data at room temperature and hence the structure determined may be dependent upon the dynamics of the system.

Acknowledgments

Part of this work was funded by the Science and Engineering Research Council. AA gratefully acknowledges the award of a postgraduate scholarship from the Ministry of Higher Education, Algeria. The authors wish to express thanks to C J Carlile, A Smith and M Prager at the ISIS Pulsed Neutron Facility, Rutherford Appleton Laboratory for valuable assistance with the INS measurements and data analysis. We are also grateful for permission from I Anderson, A Heidemann and co-workers to use their INS data from the ILL in the fitting procedure.

References

[1] Wipf H, Steinbinder D, Neumaier K, Gutsmiedl P, Magerl A and Dianoux A J 1987 *Springer Proceedings in Physics* vol 17 (Berlin: Springer) p 153 and references therein

[1a] Eckert J, Kubas G J and Dianoux A J 1988 *J. Chem. Phys.* **88** 466
[2] Clough S 1989 *J. Phys.: Condens. Matter* **1** 501
[3] Stoeckli A, Furrer A, Schoenenberger C H, Meier B H, Ernst R R and Anderson I 1986 *Physica* B **136** 161
Meier B H, Meyer R, Ernst R R, Stockli A, Furrer A, Halg W and Anderson I 1984 *Chem. Phys. Lett.* **108** 522
[4] Furic K 1984 *Chem. Phys. Lett.* **108** 518
[5] Meier B H, Graf F and Ernst R R 1982 *J. Chem. Phys.* **76** 767
[6] Nagaoka S, Terao T, Imashiro F, Saika A, Hirota N and Hayashi S 1983 *J. Chem. Phys.* **79** 4694
[7] Nagaoka S, Terao T, Imashiro F, Saika A, Hirota N and Nayashi S 1981 *Chem. Phys. Lett.* **80** 580
[8] Idziak S and Pislewski N 1987 *Chem. Phys.* **111** 439
[9] Trommsdorff H P 1987 *J. Lumin.* **38** 129
[10] Skinner J L and Trommsdorff H P 1988 *J. Chem. Phys.* **89** 897
[11] Jeener J and Broekaert P 1967 *Phys. Rev.* **157** 232
[12] Look D C and Lowe L J 1966 *J. Chem. Phys.* **44** 3437
[13] Ernst R R, Furrer A, Heidemann A, Stockli A and Schoenenberger Ch 1985 *ILL Report* 9-04-350
Ernst R R, Furrer A, Heidemann A, Stockli A and Anderson I 1986 *ILL Report* 9-04-371
[14] Ernst R R, Furrer A, Heidemann A, Meier B H, Stockli A and Anderson I 1984 *ILL Report* 9-03-351 (see also [3])
[15] Lauer O, Stehlik D and Hausser K H 1972 *J. Magn. Reson.* **6** 524
[16] Davey G and Whitlow S H 1973 *J. Cryst. Mol. Struct.* **3** 193
[17] Housty P J and Hospital M 1965 *Acta. Crystallogr.* **18** 753
[18] Feld R, Lehmann M S, Muir K W and Speakman J C 1981 *Z. Kristallogr.* **157** 215
[19] Bailey M and Brown C J 1967 *Acta. Crystallogr.* **22** 387
[20] Goedkoop J A and MacGillavry C H 1957 *Acta. Crystallogr.* **10** 125